# Metal Clips That Induce Unstructured Pentapeptides To Be Alpha Helical In Water

*Michelle T. Ma*[§], *Huy N. Hoang*[‡], *Conor C.G. Scully*[‡], *Trevor G. Appleton*[§], *David P. Fairlie*[‡]*

[§]School of Molecular and Microbial Biosciences; and [‡]Institute for Molecular Bioscience; The University of Queensland, Brisbane Qld 4072, Australia.

Correspondence to : Professor David Fairlie email: d.fairlie@imb.uq.edu.au, Tel: +61-733462989, Fax : +61-733462990

**CONTENTS**

**Figure S1**. ESI-MS of *cis*-$[Ru(NH_3)_4(1,5\text{-Ac-MARAM-NH}_2)]^{2+}$ generated in situ from *cis*-$[Ru(NH_3)_4(OH_2)_2]^{2+}$ mixed with Ac-MARAM-$NH_2$ (**1**) in water.

**Figure S2**. CD spectra of cis-$[Ru(NH_3)_4(MARAM)]^{2+}$ in TFE (0-50%) and at 5-85°C.

**Figure S3**. Temperature dependence of NMR chemical shifts for amide NH of (a) **9** and (b) **7**.

**Figure S4**. Proton NMR chemical shift differences for CHα between MARAM (**5**) and *cis*-$[Ru(NH_3)_4(MARAM)]^{2+}$ (**9**) or $[Pd(en)(MARAM)]^{2+}$ (**7**).

**Figure S5**. 500 MHz T-ROESY NMR spectrum (298 K) for **9** in acetate buffer pH 4.0.

**Figure S6**. 500 MHz T-ROESY NMR spectrum (298 K) for **7** in 90%$H_2O$:10%$D_2O$.

**Figure S7**. Proton NMR spectra for HARAH (**4**) and *in situ* complexes with *cis*-$Ru(NH_3)_4^{2+}$ (**8**) and $Pd(en)^{2+}$ (**6**) in water.

**Figure S8.** $^1H$ TOCSY NMR spectra for $C^2H$ and $C^5H$ in **6** and **8**.

**Figure S9.** $^1H$ NMR spectrum for NH and $C^2H$, $C^5H$ region of (a) MAAAH* and (b) **10**, cis-$[Ru(NH_3)_4(MAAAH*)]^{2+}$.

**Figure S10.** $^1H$ NMR spectrum for NH and $C^2H$, $C^5H$ region of (a) H*AAAM and (b) **11**, cis-$[Ru(NH_3)_4(H*AAAM)]^{2+}$.

**Figure S11.** $^1H$ NMR spectra of (a) **9**, cis-$[Ru(NH_3)_4(MARAM)]^{3+}$, (b) **10**, cis-$[Ru(NH_3)_4(MAAAH*)]^{2+}$, (c) **11**, cis-$[Ru(NH_3)_4(H*AAAM)]^{2+}$ and (d) **8**, cis-$[Ru(NH_3)_4(HARAH)]^{3+}$.

**Figure S12.** CD spectra of $[Pd(en)(MARAM)]^{3+}$ in water at pH 3.5 (black) and 7.0 (green); versus free peptide (5) at pH 4.0 (yellow).

**Figure S13.** $^{15}N$ NMR spectra for reaction between $[Pd(en)(OH_2)_2]^{2+}$ and **5** at pH 3.5 (blue), 5.5 (red), 7.5 (green) 9.5 (purple).

**Table S1.** Proton chemical shifts and $^3J_{NHH\alpha}$ for **5**, Ac-MARAM-$NH_2$, **9**, cis-$[Ru(NH_3)_4$(Ac-MARAM-$NH_2)]^{3+}$, and **7**, $[Pd(en)$(Ac-MARAM-$NH_2)]^{3+}$ in 90%H2O:10%D2O at pH 4.0.

**Table S2.** ROE, hydrogen bonding, metal binding and ϕ angle restraints used in the structure calculation for cis-$[Ru(NH_3)_4$(1,5-Ac-MARAM-$NH_2)]$, **9**.

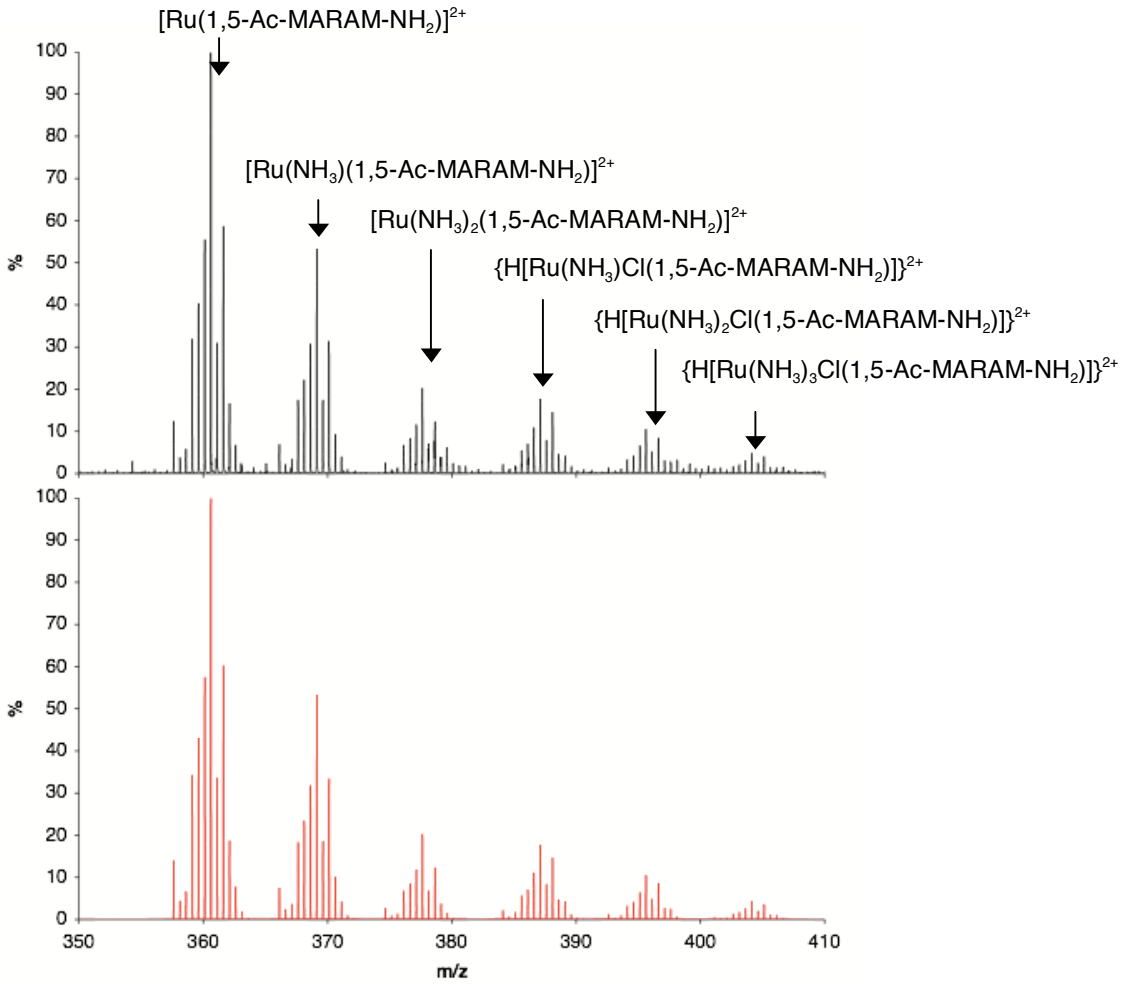


**Figure S1**. **ESI-MS of *cis*-$[Ru(NH_3)_4(1,5\text{-Ac-MARAM-NH}_2)]^{2+}$ generated in situ from *cis*-$[Ru(NH_3)_4(OH_2)_2]^{2+}$ mixed with Ac-MARAM-$NH_2$ (1) in water.** The spectrum (—, experimental; —, simulated) shows formation of a 1:1 ruthenium:peptide species. Variation in ammine and chloro ligand content and protonation state is typical of electrospray mass spectra for metallopeptides in the gas phase.

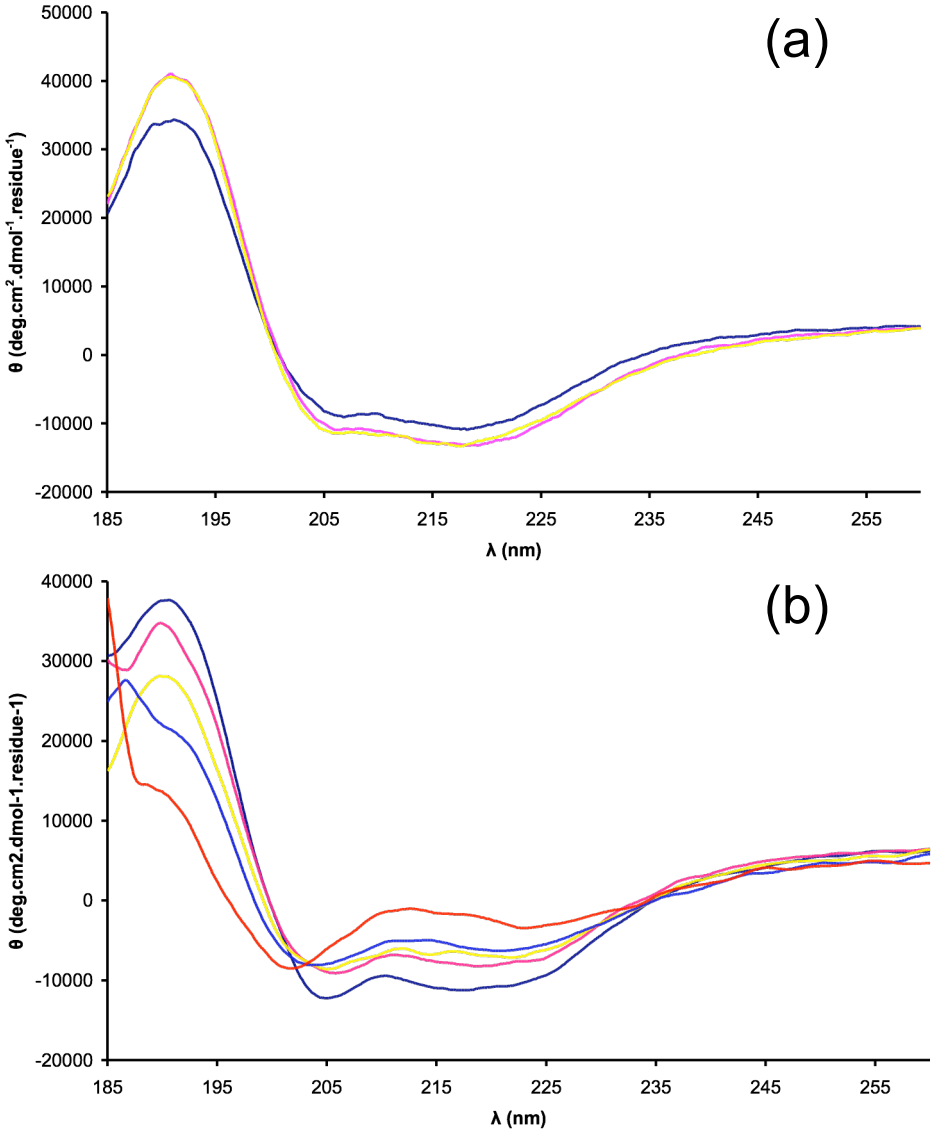


**Figure S2**. CD spectra of *cis*-$[Ru(NH_3)_4(MARAM)]^{2+}$ (**9**) in (a) TFE 0% (—), 20% (—), 50% (—); and (b) at 5 (—), 25 (—), 45 (—), 65 (—) and 85 (—) °C.

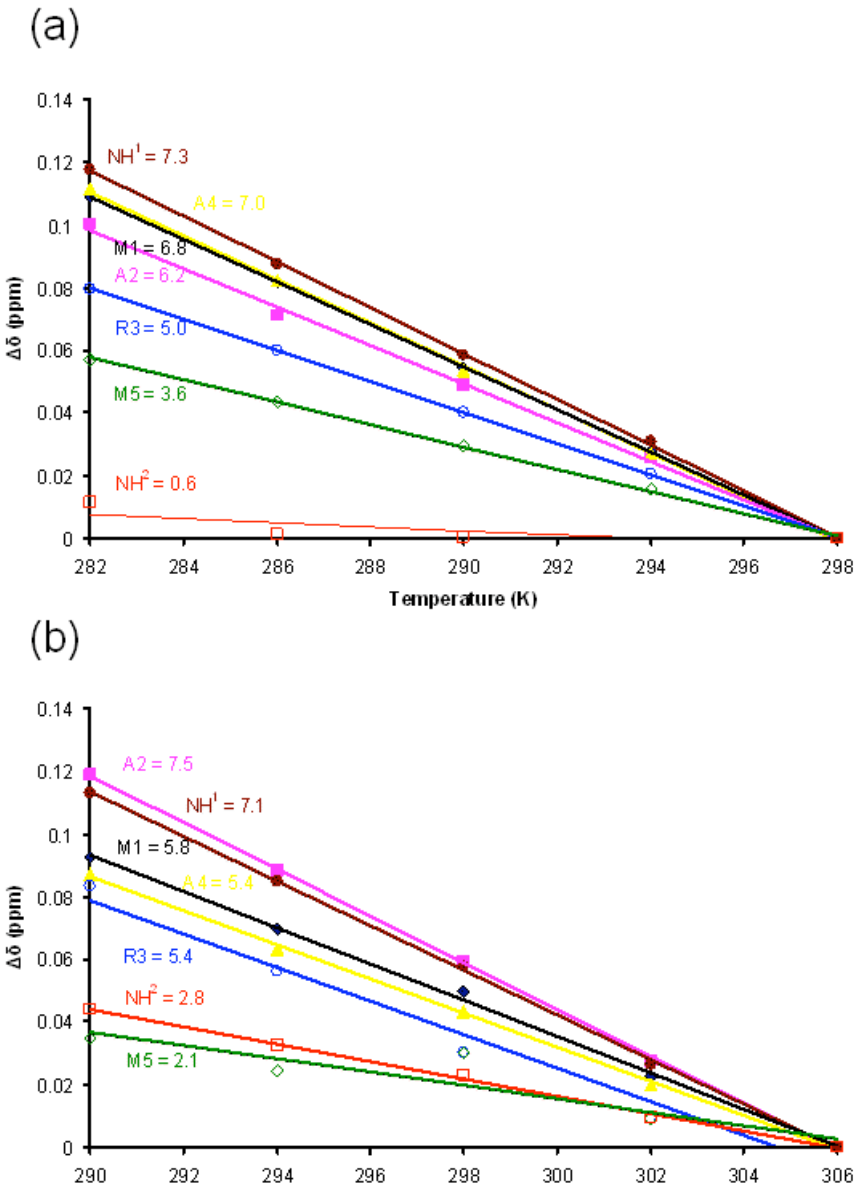


**Figure S3**. **Temperature dependence of NMR chemical shifts for amide NH of (a) 9 and (b) 7.** Line slopes indicating temperature coefficients (Δδ/T, ppb/K) for each residue are shown.

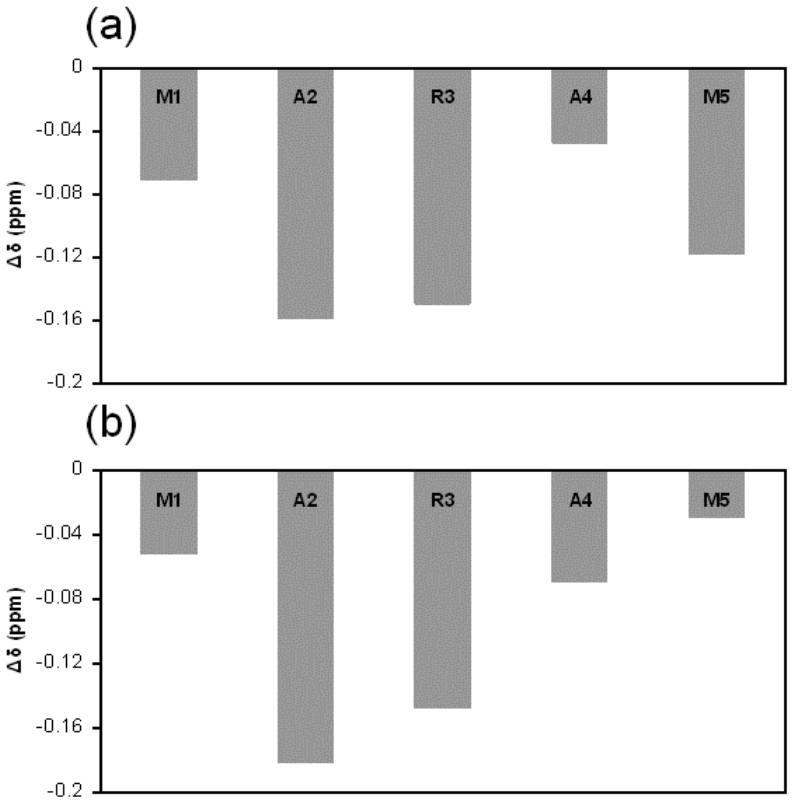


**Figure S4**. **Proton NMR chemical shift differences for CHα between MARAM (5) and *cis*-[Ru(NH$_3$)$_4$(MARAM)]$^{2+}$ (9) or [Pd(en)(MARAM)]$^{2+}$ (7).** (a) Deviations of CHα between **9** and **5**, Δδ = δ CHα(**9**) - δ CHα(**5**) in 90% $H_2O$ 10% $D_2O$. (b) Deviations of CHα chemical shifts between **7** and **5**, Δδ = δ CHα(**7**) - δ CHα(**5**) in 90% $H_2O$ 10% $D_2O$. Negative values indicate upfield shifts for **9** or **7** versus **5** and are typical of α-helicity.

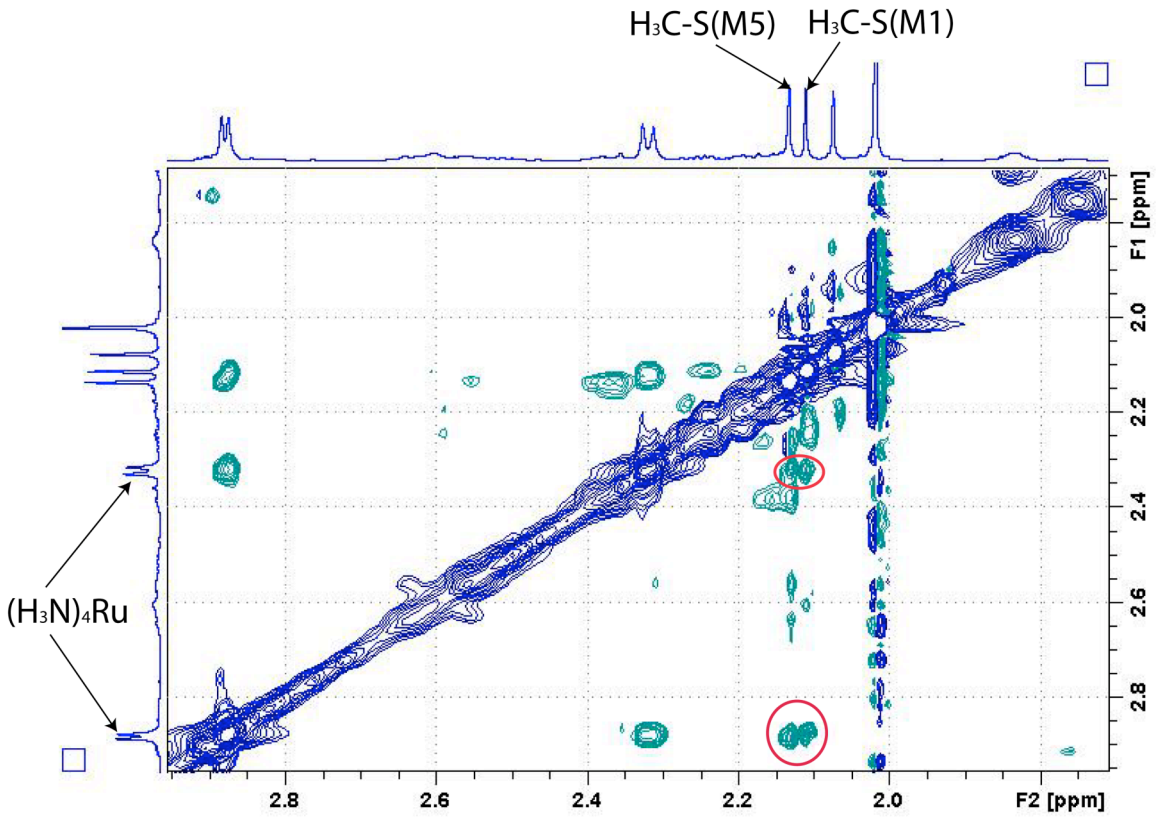


**Figure S5**. **500 MHz T-ROESY NMR spectrum (298 K) for 9 in acetate buffer pH 4.0.** Mixing time 350 ms, spin-lock 16dB (3kHz). NOEs between cis-$[Ru(NH_3)_4(OH_2)_2]^{2+}$ and two methionine side chains are shown as red circles.

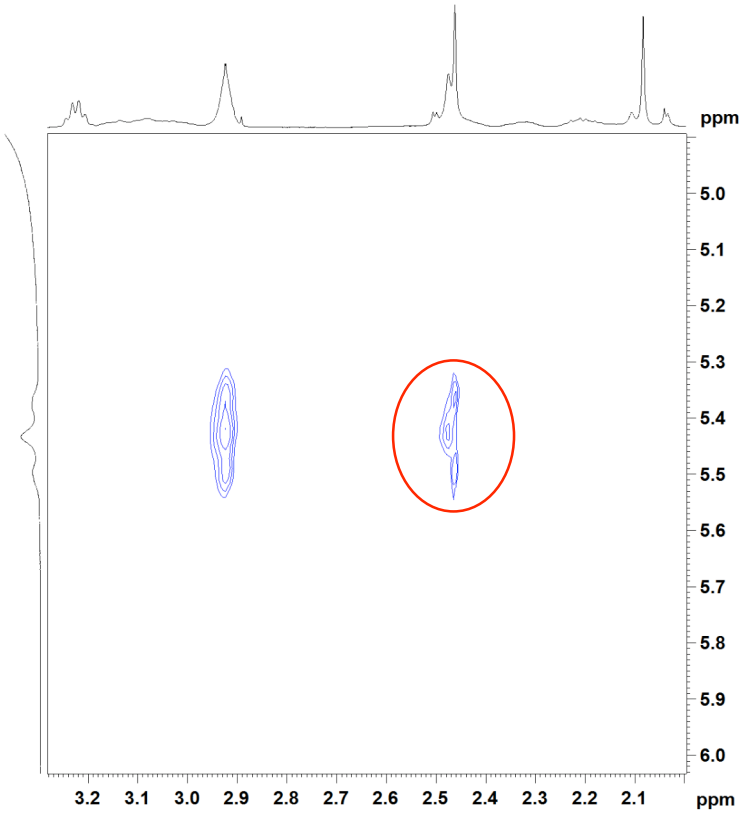


**Figure S6**. **500 MHz T-ROESY NMR spectrum (298 K) for 7 in 90%$H_2O$:10%$D_2O$.** Mixing time 350 ms, spin-lock 16dB (3kHz)). ROEs between Pd(en) and two S-$CH_3$ protons of the methionine side chains are shown in red.

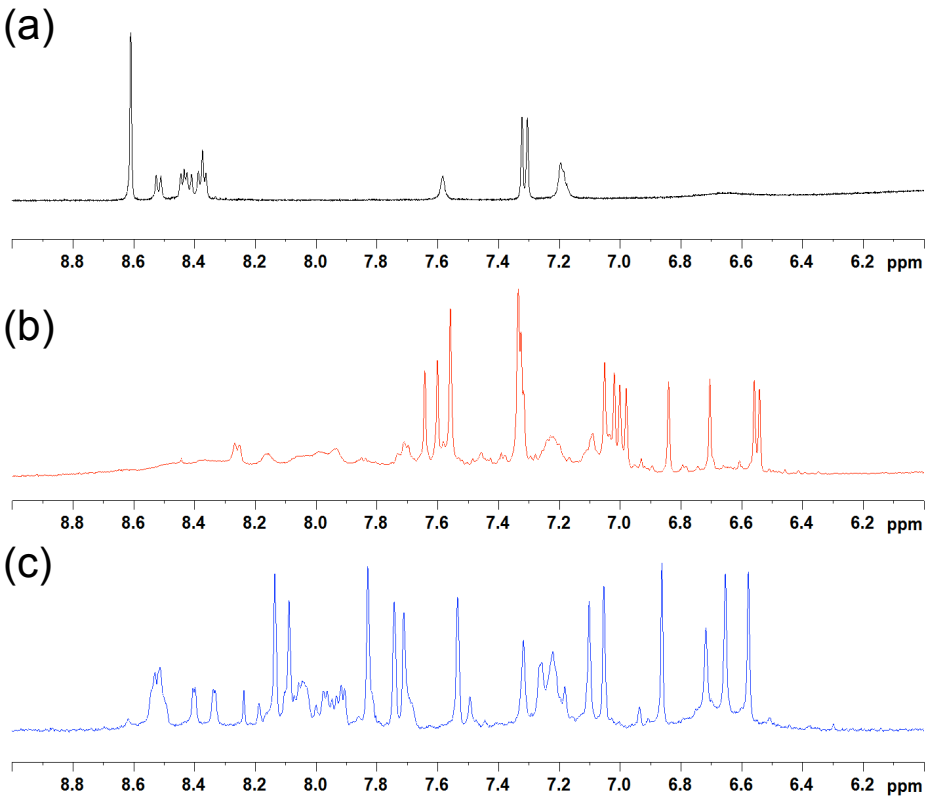


**Figure S7**. **Proton NMR spectra for HARAH (4) and *in situ* complexes with cis-$[Ru(NH_3)_4(OH_2)_2]^{2+}$ (8) and $[Pd(en)(OH_2)_2]^{2+}$ (6) in water**. **(a)** $^1$H NH region of **4**, HARAH, ($D_2O/H_2O$ 10%/90%, pH 4), showing each set of $C^2H$ and $C^5H$ peaks at 8.608 and 7.321 ppm; and 8.608 and 7.304 ppm respectively. **(b)** $^1$H NH region of **8**, cis-$[Ru(NH_3)_4(HARAH)]^{3+}$, ($D_2O/H_2O$ 10%/90%, pH 6) and **(c)** $^1$H NH region of **6**, $[Pd(en)(HARAH)]^{3+}$, ($D_2O/H_2O$ 10%/90%, pH 4). Multiple $C^2H$ and $C^5H$ signals in the $^1$H spectra of **8** and **6** indicate formation of several linkage isomers. $C^2H$ and $C^5H$ peaks of **8** and **6** display dramatic upfield shifts relative to free peptide, **4**, indicative of ruthenium and palladium binding to N atoms of the imidazole side chains respectively.

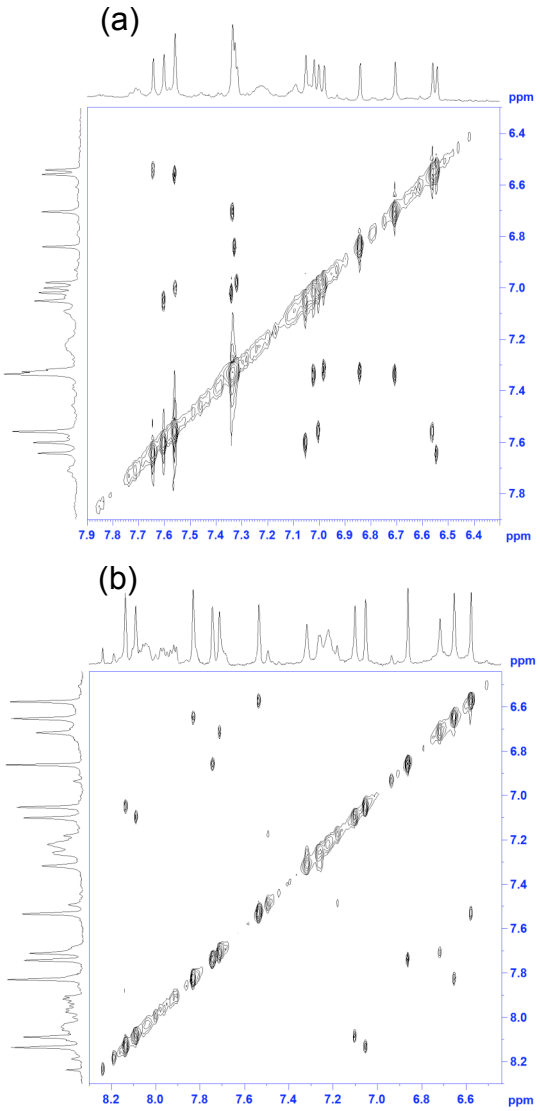


**Figure S8. $^{1}$H TOCSY NMR spectra for C$^{2}$H and C$^{5}$H in 8 and 6.** (a) **8**, cis-$[Ru(NH_3)_4(HARAH)]^{2+}$, ($D_2O/H_2O$ 10%/90%, pH 6). There are eight sets of peaks indicative of four linkage isomers: (C$^{2}$H, C$^{5}$H) at (7.642, 6.541), (7.602, 7.050), (7.557, 7.000), (7.557, 6.559), (7.334, 7.019), (7.334, 6.704), (7.326, 6.840), (7.316, 6.979) ppm. (b) **6**, $[Pd(en)(HARAH)]^{2+}$, ($D_2O/H_2O$ 10%/90%, pH 4) showing six sets of peaks indicative of three linkage isomers: (C$^{2}$H, C$^{5}$H) at (8.137, 7.047), (8.090, 7.095), (7.831, 6.650), (7.743, 6.857), (7.713, 6.715), (7.537, 6.572) ppm.

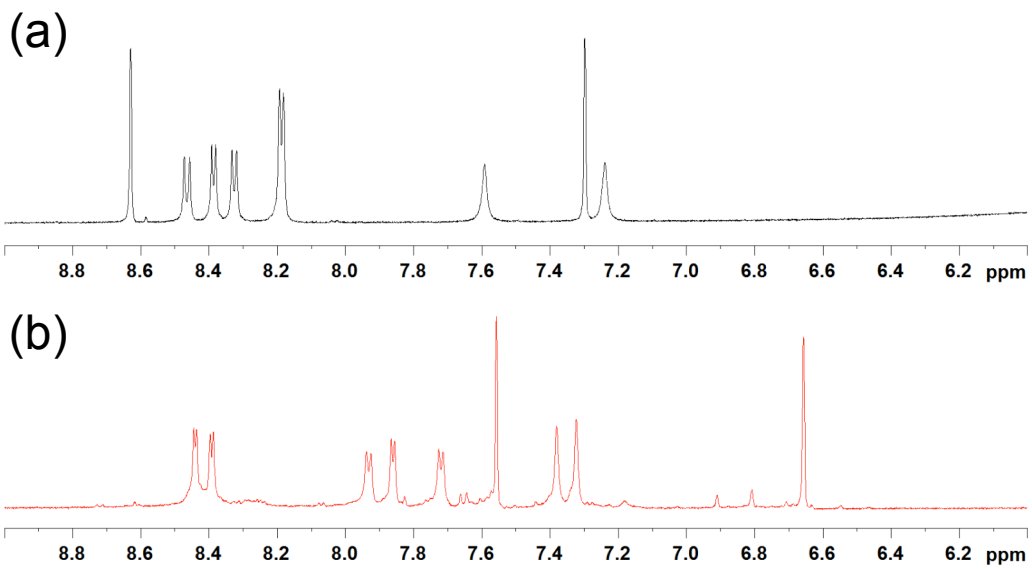


**Figure S9. $^{1}$H NMR spectrum for NH and C$^{2}$H, C$^{5}$H region of (a) MAAAH* and (b) 10, cis-[Ru(NH$_3$)$_4$(MAAAH*)]$^{2+}$.** C$^{2}$H and C$^{5}$H peaks shift respectively from 8.630 and 7.299 ppm to 7.557 and 6.657 ppm upon ruthenium binding. Amide NH resonances disperse upon ruthenium binding.

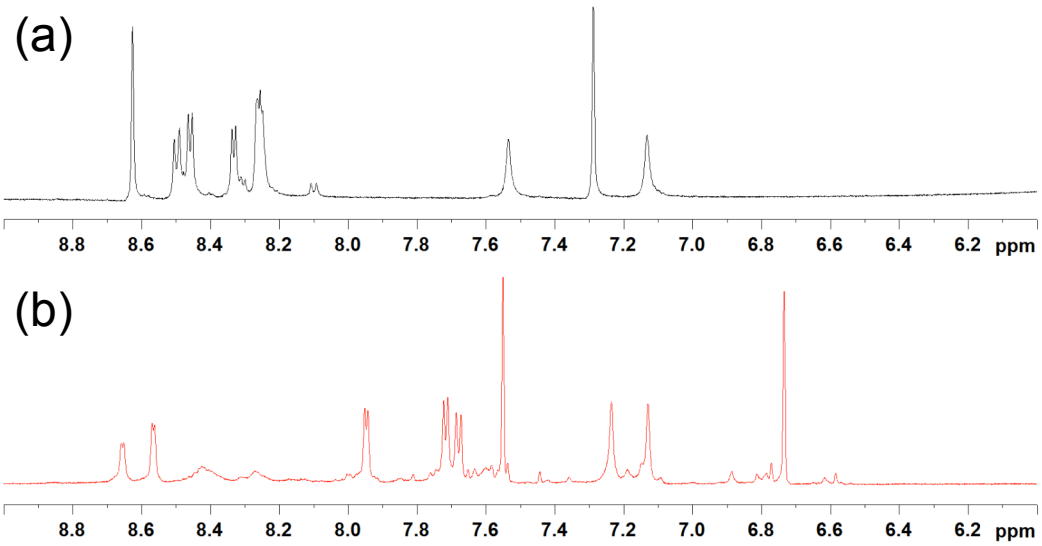


**Figure S10. $^{1}$H NMR spectrum for NH and C$^{2}$H, C$^{5}$H region of (a) H*AAAM and (b) 11, cis-[Ru(NH$_3$)$_4$(H*AAAM)]$^{2+}$.** C$^{2}$H and C$^{5}$H peaks shift respectively from 8.625 and 7.289 ppm to 7.551 and 6.734 ppm upon ruthenium binding. Amide NH resonances disperse upon ruthenium binding.

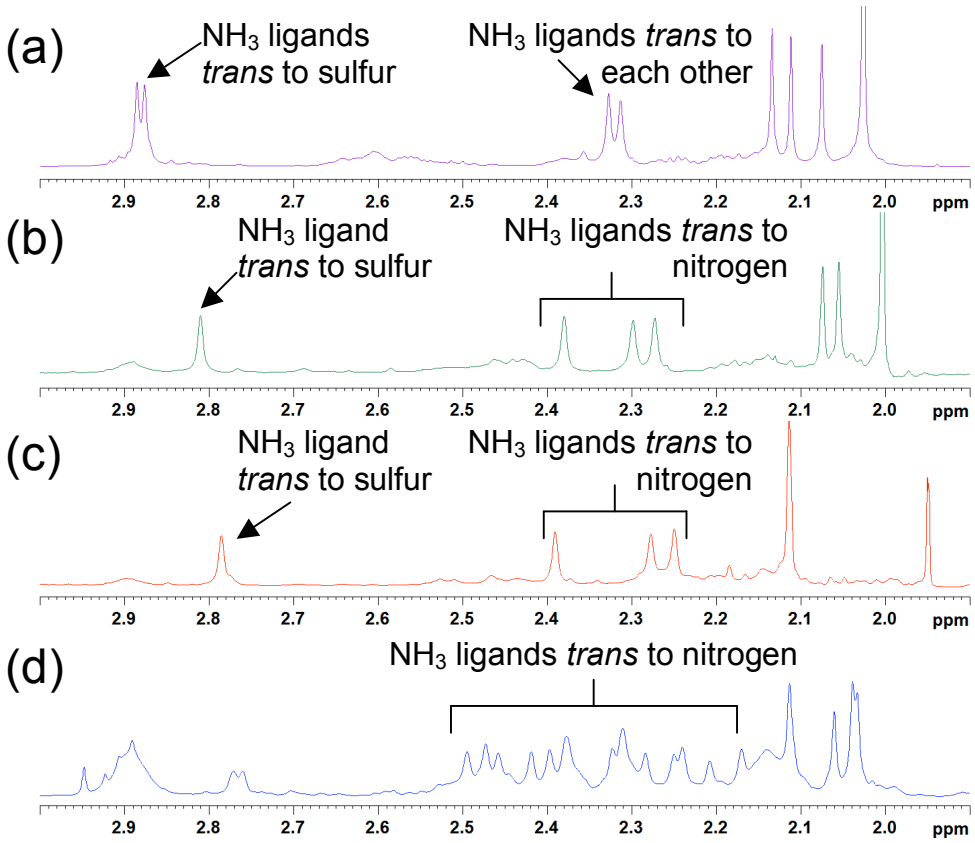


**Figure S11: $^{1}$H NMR spectra of (a) 9, cis-[Ru(NH$_3$)$_4$(MARAM)]$^{32+}$, (b) 10, cis-[Ru(NH$_3$)$_4$(MAAAH*)]$^{2+}$, (c) 11, cis-[Ru(NH$_3$)$_4$(H*AAAM)]$^{2+}$ and (d) 8, cis-[Ru(NH$_3$)$_4$(HARAH)]$^{2+}$.** $^{1}$H NMR spectra of **9**, **10** and **11** all display four signals corresponding to the four ammine ligands of the [Ru(NH$_3$)$_4$]$^{2+}$ clip. Ammine ligands *trans* to *S*-donor ligands (of methionine side chains) occur between 2.75 and 2.9 ppm. As **10** and **11** have only one coordinated methionine, only one signal is observed in this region. Ammine ligands *trans* to *N*-donor ligands (of the [Ru(NH$_3$)$_4$]$^{2+}$ clip and/or the histidine side chains) occur between 2.2 and 2.5 ppm. **9** coordinates to the peptide exclusively through methionine residues and therefore ammine signals between 2.2 and 2.5 correspond to the two ammine ligands *trans* to each other. Because **8** is a mixture of four linkage isomers, numerous signals (at least 10 – 12) corresponding to ammine ligands *trans* to *N*-donor ligands are observed between 2.2 and 2.5 ppm. No *S*-donor atoms are present in **8**, and so no ammine signals are observed between 2.75 and 2.9 ppm.

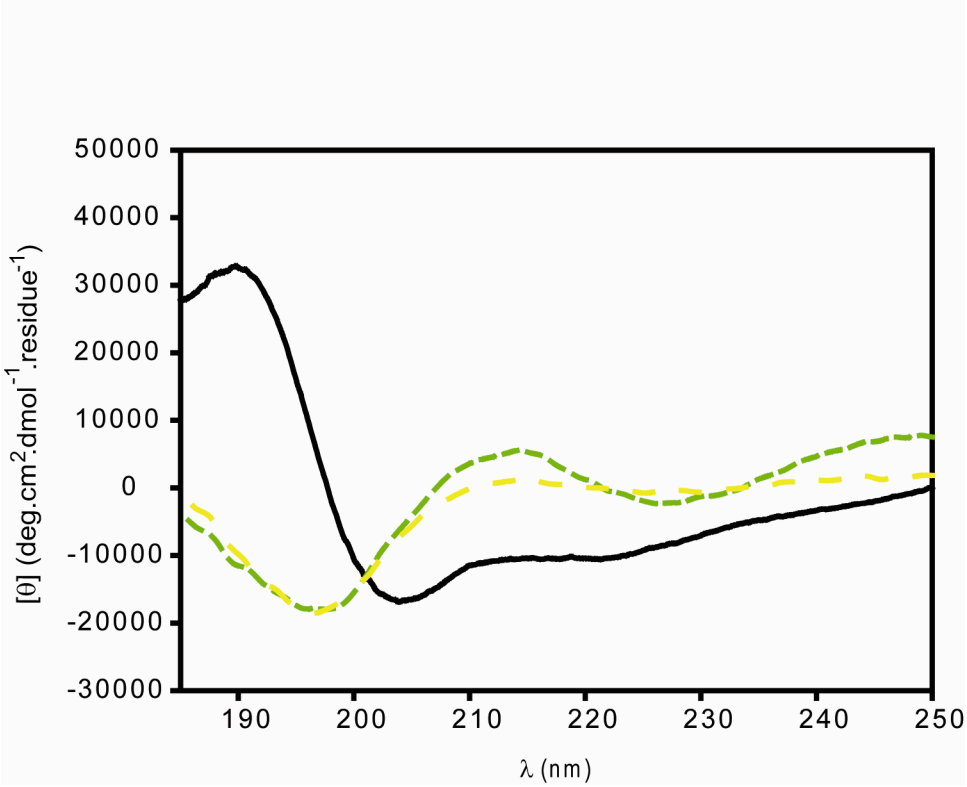


**Figure S12. CD spectra of [Pd(en)(MARAM)]$^{3+}$ in water at pH 3.5 (black) and 7.0 (green); versus free peptide (5) at pH 4.0 (yellow).**

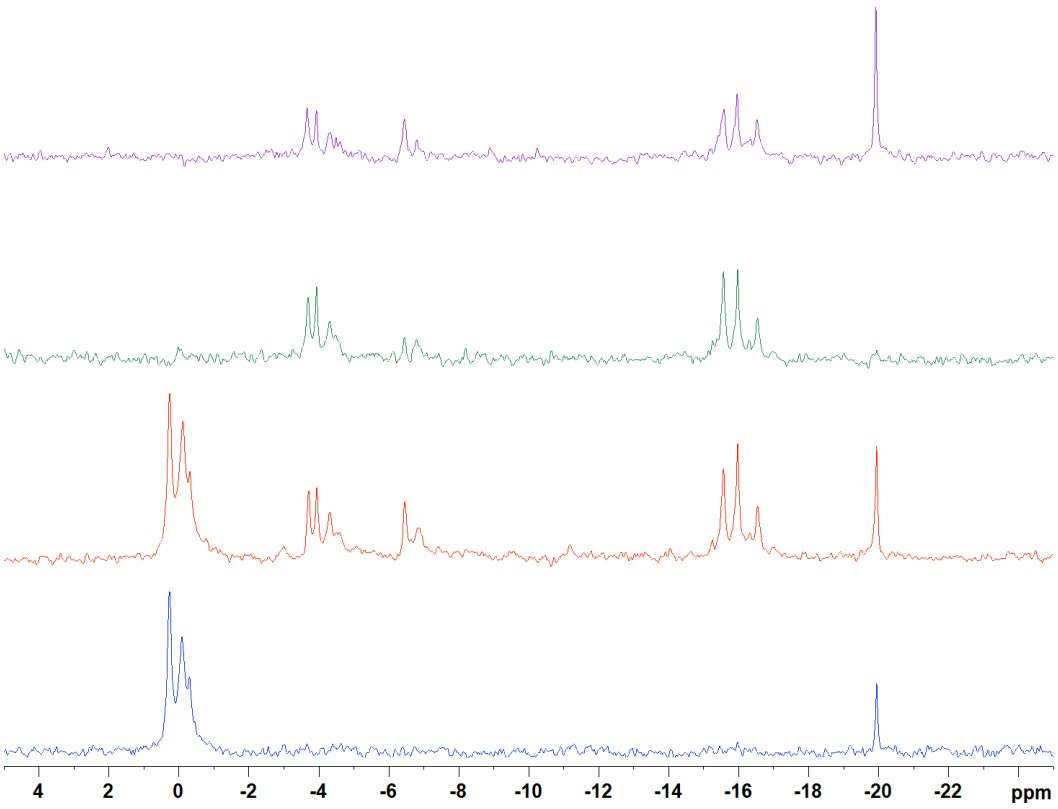


**Figure S13: $^{15}$N NMR spectra for reaction between $[Pd(en)(OH_2)_2]^{2+}$ and 5 at pH 3.5 (blue), 5.5 (red), 7.5 (green) 9.5 (purple).** At pH 3.5, the peptide is bound to $[Pd(en)]^{2+}$ through sulfur donors. (Signals for $^{15}$N nuclei *trans* to sulfur donors are between 0 and -10 in the $^{15}$N NMR spectrum.) As pH is increased, nitrogen atoms on the peptide compete for metal binding, possibly forming 5- and 6-membered chelate rings. (Signals for $^{15}$N nuclei *trans* to nitrogen donors are between -10 and -20 in the $^{15}$N NMR spectrum.) The signal at -20 ppm corresponds to $[Pd(en)(solvent)_2]^{2+}$.

**Table S1. Proton chemical shifts and $^3J_{NHH(}$ for 5, Ac-MARAM-$NH_2$, 9, cis-$[Ru(NH_3)_4$(Ac-MARAM-$NH_2)]^{3+}$, and 7, $[Pd(en)$(Ac-MARAM-$NH_2)]^{3+}$ in 90%H2O:10%D2O at pH 4.0.**

| **Atom** | Ac-MARAM-$NH_2$(**5**) | | Ru(Ac-MARAM-$NH_2$)(**9**) | | Pd(Ac-MARAM-$NH_2$)(**7**) |
|---|---|---|---|---|---|
| | Chemical Shift(ppm) | $^3J_{NHH□}$ (Hz) | Chemical Shift(ppm) | $^3J_{NHH□}$ (Hz) | Chemical Shift(ppm) |
| **Ac** | | | | | |
| $CH_3$ | 2.03 | | 2.08 | | 2.08 |
| **M1** | | | | | |
| NH | 8.30 | 7.8 | 8.44 | 4.5 | 8.54 |
| CH(□) | 4.39 | | 4.31 | | 4.33 |
| $CH_2$(□) | 1.99 | | 2.15 | | 2.32, 3.21 |
| $CH_2$(□) | 2.58 | | 2.60 | | 3.01, 3.14 |
| S-$CH_3$ | 2.11 | 7.7 | 2.11 | | 2.48 |
| **A2** | | | | | |
| NH | 8.39 | 5.6 | 8.66 | 3.9 | 8.65 |
| CH(□) | 4.29 | | 4.13 | | 4.11 |
| $CH_3$(□) | 1.38 | | 1.41 | 7.6 | 1.42 |
| **R3** | | | | | |
| NH | 8.25 | 6.7 | 7.92 | 5.5 | 7.95 |
| CH(□) | 4.28 | | 4.13 | | 4.13 |
| $CH_2$(□) | 1.77 | | 1.84 | | 1.85 |
| $CH_2$(□) | 1.63 | | 1.66 | | 1.65 |
| $CH_2$(□) | 3.21 | | 3.22 | | 3.22 |
| NH(□) | 7.19 | | 7.21 | | 7.21 |
| **A4** | | | | | |
| NH | 8.33 | 5.6 | 8.03 | 5.7 | 8.04 |
| CH(□) | 4.31 | | 4.26 | | 4.24 |
| $CH_3$(□) | 1.40 | 7.7 | 1.43 | 7.5 | 1.44 |
| **M5** | | | | | |
| NH | 8.33 | 7.5 | 8.00 | 7.3 | 7.95 |
| CH(□) | 4.43 | | 4.31 | | 4.40 |
| $CH_2$(□) | 2.01 | | 2.38, 2.14 | | 2.43, 2.18 |
| $CH_2$(□) | 2.59 | | 2.64, 2.55 | | 3.08 |
| S-$CH_3$ | 2.11 | | 2.13 | | 2.46 |
| $NH_2$ (terminal) | 7.14, 7.55 | | 7.26, 7.27 | | 7.31, 7.23 |

**Table S2. ROE, hydrogen bonding, metal binding and ϕ angle restraints used in the structure calculation for cis-$[Ru(NH_3)_4(1,5\text{-Ac-MARAM-}NH_2)]^{2+}$, 9.**

| Atom A | Atom B | Restraint |
|---|---|---|
| Ac $CH_3$ | M1 NH | Weak + correction, 6.0 Å |
| Ac $CH_3$ | M1 $CH_3\beta$ | Medium + correction, 6.0 Å |
| Ac $CH_3$ | A2 NH | Very Weak, 6.0 Å |
| Ac $CH_3$ | R3 NH | Very Weak, 6.0 Å |
| Ac $CH_3$ | A4 NH | Very Weak, 6.0 Å |
| M1 CHα | M1 NH | Medium, 3.5 Å |
| M1 CHα | A2 NH | Medium, 3.5 Å |
| M1 CHα | A4 NH | Very Weak, 6.0 Å |
| M1 NH | A2 NH | Medium, 3.5 Å |
| M1 $CH_2\beta$ | A2 NH | Very Weak, 6.0 Å |
| M1 $CH_2\beta$ | M1 NH | Strong + correction, 3.7 Å |
| M1 $CH_2\beta$ | M1 CHα | Medium + correction, 4.5 Å |
| M1 $CH_2\gamma$ | M1 CHα | Medium + correction, 4.5 Å |
| M1 $CH_2\gamma$ | A2 $CH_3\beta$ | Very Weak, 6.0 Å |
| M1 $CH_3\varepsilon$ | M5 $CH_3$ | Medium + correction, 6.0 Å |
| A2 CHα | A2 NH | Medium, 3.5 Å |
| A2 NH | R3 NH | Medium, 3.5 Å |
| A2 $CH_3\beta$ | R3 NH | Medium,+ correction, 5.0 Å |
| A2 $CH_3\beta$ | A2 NH | Medium + correction, 5.0 Å |
| A2 $CH_3\beta$ | A2 CHα | Strong + correction, 4.2 Å |
| A2 $CH_3\beta$ | M5 $CH_2\gamma$ | Very Weak, 6.0 Å |
| A2 $CH_3\beta$ | M5 $CH_2\beta$ | Very Weak, 6.0 Å |
| R3 CHα | R3 NH | Medium, 3.5 Å |
| R3 CHα | A4 NH | Medium, 3.5 Å |
| R3 CHα | M5 $CH_2\beta$ | Very Weak, 6.0 Å |
| R3 NH | A4 NH | Medium, 3.5 Å |
| R3 NH | R3 $CH_2\gamma$ | Weak + correction, 6.0 Å |

| | | |
|---|---|---|
| R3 $CH_2\beta$ | R3 NH | Strong + correction, 3.7 Å |
| R3 $CH_2\beta$ | A4 NH | Medium + correction, 4.5 Å |
| R3 $CH_2\beta$ | A4 CHα | Very Weak, 6.0 Å |
| R3 $CH_2\gamma$ | R3 $CH_2\beta$ | Strong + correction, 4.7 Å |
| R3 $CH_2\gamma$ | A4 CHα | Very Weak, 6.0 Å |
| R3 $CH_2\delta$ | R3 $CH_2\beta$ | Weak + correction, 6.0 Å |
| R3 $CH_2\delta$ | R3 $CH_2\gamma$ | Strong + correction, 4.7 Å |
| R3 $CH_2\delta$ | R3 NH ε | Strong + correction, 3.7 Å |
| R3 NHε | R3 $CH_2\beta$ | Weak + correction, 6.0 Å |
| R3 NHε | R3 $CH_2\gamma$ | Medium + correction, 4.5 Å |
| A4 CHα | A4 NH | Medium, 3.5 Å |
| A4 CHα | M5 NH | Medium, 3.5 Å |
| A4 $CH_3\beta$ | M5 NH | Weak + correction, 6.0 Å |
| A4 $CH_3\beta$ | A4 CHα | Strong + correction, 4.2 Å |
| A4 $CH_3\beta$ | A4 NH | Medium + correction, 5.0 Å |
| M5 CHα | M5 NH | Medium, 3.5 Å |
| M5 CHα | $NH_2$ | Medium + correction, 4.5 Å |
| M5 CHα | M5 $CH_2\beta$ | Strong + correction, 3.7 Å |
| M5 CHα | M5 $CH_2\gamma$ | Medium + correction, 4.5 Å |
| M5 NH | $NH_2$ | Medium + correction, 4.5 Å |
| M5 $CH_2\beta$ | $NH_2$ | Weak + correction, 6.0 Å |
| M1, S | M5, S | Metal coordination, 3.4 Å |
| M1, CO | M5, NH | Hydrogen bond, 1.88 |
| M1, CO | M5, N | Hydrogen bond, 2.88 |
| A2, CO | $NH_2$ | Hydrogen bond, 1.88 |
| A2, CO | N (C-terminus) | Hydrogen bond, 2.88 |

| Residue | Angle | Restraint |
|---|---|---|
| M1 | CO-N-Cα-CO | -65.0±30º |
| A2 | CO-N-Cα-CO | -65.0±30º |
| R3 | CO-N-Cα-CO | -65.0±30º |
| A4 | CO-N-Cα-CO | -65.0±30º |